

# A Numerical Simulation of Turbulent Non-premixed Counter-flow Syngas-air Flames Structure and NO Emissions

**Khadidja Safer, Meriem Safer**

Laboratoire des Carburants Gazeux et de l'Environnement, Faculté du Génie Mécanique,  
Université des Sciences et de la Technologie d'Oran Mohamed Boudiaf, BP. 1505  
Elmenaouer, Oran 31000, Algérie

**Fouzi Tabet**

European Institute for Energy Research (EIFER) - EDF R&D, Emmy-Noether-Strasse 11, D-76131 Karlsruhe, Germany

**Brahim Sarh, Iskender Gökcalp**

Institut de Combustion, Aérothermique, Réactivité et Environnement (ICARE), Centre National de la Recherche Scientifique (CNRS), 1C avenue de la recherche scientifique, Orléans 45071 Cedex 2, France

Key words: Turbulence, Flame structure, Diffusion flame, Counter-flow, Syngas, NO<sub>x</sub> emissions

## Abstract

This study reports results from numerical investigations of flame structure and emissions of a turbulent non-premixed opposed syngas/air flame over a wide range of hydrogen percentage (H<sub>2</sub>/CO ratio between 0.4 and 2.0) and operating pressure (1 – 10 atm).

Numerical model is based on RANS technique and axisymmetric formulation. It includes a *k*-epsilon turbulence model and flamelet approach of the joint scalar probability density function (PDF). Radiation effects are also considered.

Computational results showed that flame structure and emissions are impacted by syngas composition and ambient pressure. Temperature increases when H<sub>2</sub>/CO molar fraction increases. Optimum operating conditions of turbulent syngas opposed-jet flames are determined for practical industrial burners in order to reach stability and acceptable level of pollutant emissions. Hydrogen-rich syngas flames produce more NO<sub>x</sub> at lower strain rates while NO<sub>x</sub> levels increase towards hydrogen-lean syngas flames at higher strain rates.

## 1 Introduction

Turbulent counterflow flame represents a very useful benchmark of complexity intermediate between laminar flames and practical systems. By operating in a turbulent Reynolds number regime of relevance to practical systems such as gas turbines and internal combustion engines, it retains the interaction of turbulence and chemistry of such environments, but offers several advantages including: (a) the achievement of high Reynolds numbers without pilot flames, which is particularly advantageous from a modelling standpoint; (b) control of the transition from stable flames to local extinction/reignition conditions; (c) compactness of the domain by comparison with jet flames, with obvious advantages from both a diagnostic and, especially, a computational viewpoint; and (d) the reduction or, altogether, elimination of soot formation, thanks to the high strain rates and low residence times of such a system, and the establishment of conditions of large stoichiometric mixture fraction, as required for robust flame stabilization.

Syngas counterflow flames have been extensively studied under laminar conditions. Drake and Blint [1] numerically investigated the effect of flame stretch on the flame structure and NO<sub>x</sub> formation in opposed-flow diffusion flames with CO/H<sub>2</sub>/N<sub>2</sub> mixture as a fuel. They showed that flame structure is very sensitive to H<sub>2</sub> amount and NO concentration decreased dramatically as flame stretch increased. Park *et al.* [2] conducted a numerical study to understand the impact of fuel composition on flame structure in H<sub>2</sub>/CO synthetic gas diffusion flame with and without CO<sub>2</sub> dilution at atmospheric pressure and noticed that fractional flame temperature loss by flame radiation increased as CO and CO<sub>2</sub> mole fractions increased. Giles *et al.* [3] examined the effect of air-stream dilution on flame structure and NO<sub>x</sub> emission of syngas diffusion flames for two representative syngas mixtures with equal molar percentage of CO/H<sub>2</sub> and three diluents, N<sub>2</sub>, H<sub>2</sub>O and CO<sub>2</sub>. Results indicated that syngas flames with CO<sub>2</sub> and H<sub>2</sub>O dilution are more effective in reducing NO<sub>x</sub> emission

The effects of syngas composition (20% H<sub>2</sub> and 80% CO and 80% H<sub>2</sub> and 20% CO), strain rate, ambient pressure (up to 5 atm), and dilution gases on the flame structures and extinction limits of H<sub>2</sub>/CO synthetic mixture flames are analyzed by Shih *et al.* [4]. Their results indicated that flame structures and flame extinction are impacted by the composition of syngas mixture significantly. Somer *et al.* [5] presented a numerical and experimental investigation of the combustion and NO<sub>x</sub> characteristics of syngas laminar flames taking three ranges of H<sub>2</sub>/CO molar fractions and for partially premixed flames taking a wider range of syngas composition. In another study, Shih *et al.* [6] characterized NO<sub>x</sub> reactions pathways in syngas counter-flow diffusion flames for different syngas composition, pressure (up to 5 atm) and dilution percentages. Zeldovich route is demonstrated to be the main NO formation route and increasing pressure led to an enhancement of NO formation reactions, especially through Zeldovich mechanisms. Recently, a couple of investigations have been carried out on syngas jet flames in gas turbine conditions. The main reason for the growing interest in this topic is due to the development of a fuel flexible advanced gas turbine for IGCC. These works are usually performed in the framework of a research program initiated by gas turbine manufacturers [7] [8] [9] to evaluate the reliability of the components including the burner designed for natural gas operation.

The majority of modelling investigations reported above focused on laminar flames, and did not provided sufficient details about flame characteristics with respect to a wide composition of syngas fuel mixtures and a wide range of pressures.

The objective of the present work is to perform RANS simulations over a wide range of syngas fuel mixtures and operating pressure and extract information from the numerical databases to analyse flame structure and emissions in the context of turbulent non-premixed counter-flow syngas flames. The calculations are performed in the opposed-jets configuration of Geyer [10] using a wide range of molar fractions of H<sub>2</sub>/CO (i.e. 0.4, 0.8, 1, 1.4 and 2) and operating pressure (from 1 to 10 atm).

## 2 Mathematical modeling

### 2.1. Governing equations

The steady Reynolds-averaged Navier-Stokes (RANS) approach is applied. Favre averages are used to account for variable-density effects. Combustion model considered here is flamelet approach developed by Pitsch and Peters [11]:

$$\rho \frac{\partial Y_n}{\partial t} = \frac{1}{2} \rho \chi \frac{\partial^2 Y_n}{\partial Z^2} + \dot{\omega}_n \quad (1)$$

$$\rho \frac{\partial T}{\partial t} = \frac{1}{2} \rho \chi \frac{\partial^2 T}{\partial Z^2} - \frac{1}{c_p} \sum_k H_n \dot{\omega}_n + \frac{1}{2c_p} \rho \chi \left[ \frac{\partial c_p}{\partial Z} + \sum_n c_{p,n} \frac{\partial Y_n}{\partial Z} \right] \frac{\partial T}{\partial Z} \quad (2)$$

The notation in Equations (1) and (2) is as follows:  $Y_n$ ,  $T$ ,  $\rho$  are the  $n$ th species mass fraction, temperature and density, respectively.  $Le_n$  is the Lewis number of the  $n$ th species defined as  $Le_n = \lambda / (\rho D_{nm} c_{p,n})$  where  $D_{nm}$  is the multi-component ordinary diffusion coefficient,  $\dot{\omega}_n$  is the  $n$ th species reaction rate and  $\chi$  is the instantaneous scalar dissipation rate defined by:  $\chi = 2D_Z (\nabla Z \cdot \nabla Z)$ . Its modelling is based on the relation below which is taken from the counter-flow geometry [11]:

$$\chi = \chi_{st} \frac{\Phi}{\Phi_{st}} \frac{g(Z)}{g(Z_{st})} \quad (3)$$

$\chi_{st}$  is the scalar dissipation rate at stoichiometry and  $\Phi$  is a factor introduced in order to include the effect of density variation:

$$\Phi = \frac{1}{4} \frac{3(\sqrt{\rho_\infty / \rho} + 1)^2}{2\sqrt{\rho_\infty / \rho} + 1} \quad (4)$$

The subscript  $\infty$  means the oxidizer stream. The function  $g(Z)$  is given as follows [12]:

$$g(Z) = \exp[-2(\text{erfc}^{-1}(2Z))^2] \quad (5)$$

where  $\text{erfc}^{-1}$  is the inverse of the complementary error function.

Radiation is accounted for by the DO (Discrete Ordinate) model in which the RTE (Radiative Transfer Equation) is solved for a finite number of discrete solid angles [13] [14]. The heat source by radiation is given by:

$$S_h = \alpha \left( \int_{4\pi} I(r, \Omega) d\Omega - \sigma T^4 \right) \quad (6)$$

Where  $I(r, \Omega)$  is the radiation intensity, which is a function of position and direction.  $\alpha$  and  $\sigma$  are the absorption coefficient [13] and the Stephan Boltzman constant respectively.

### 2.2. Numerical details

The configuration of Geyer et al. [10] is retained for the simulations. The experiment consisted of two identical vertical opposed jets. The distance between the two nozzles was 30 mm. Air stream emanated from the upper nozzle with a bulk velocity of  $3.4 \text{ m.s}^{-1}$  while methane was injected from the lower nozzle with a bulk velocity of  $3.54 \text{ m.s}^{-1}$ . Accordingly, the bulk strain rate was  $231 \text{ s}^{-1}$ . The ambient pressure was set to 1 atm. First, model validation in the experimental configuration of Geyer et al. [10] is conducted followed by a numerical simulation of syngas flames structures and emissions. Five  $\text{H}_2/\text{CO}$  molar fractions are considered: 0.4, 0.8, 1, 1.4 and 2.0 at the pressure range between 1 and 10 atm (table 1). The calculations have been performed with FLUENT CFD code with DRAKE67 mechanism. The inlet momentum of oxidizer and fuel were taken equal.

Table 1: Syngas composition

$\text{H}_2/\text{CO}$	$\text{H}_2$	$\text{CO}$
0.4	0.29	0.71
0.8	0.45	0.55
1.0	0.50	0.50
1.4	0.583	0.417
2.0	0.67	0.33

### 3 Results

The model accuracy has been assessed using the experimental results of Geyer [10]. It was shown that flame structure is sufficiently well described. In addition, heat losses due to radiation were found to be modelled satisfactorily since the maximum flame temperatures are predicted well. Figures 1 and 2 showed a comparison between predictions and experiments in the case of axial velocity (Fig. 1) and mixture fraction (Fig. 2). Reasonable agreement was obtained at this flame conditions.

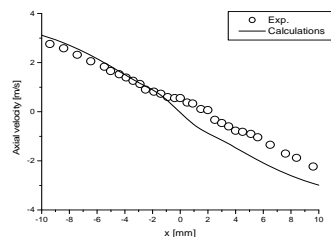


Figure 1. Axial profiles of velocity

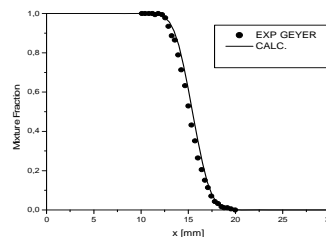


Figure 2. Axial profiles of mixture fraction

The effect of varying  $\text{H}_2/\text{CO}$  ratio on flame structure and NO emissions was afterwards investigated. Scalar and dynamic fields were calculated for  $\text{H}_2/\text{CO} = 0.4 - 2$  in the pressure range between 1 and 10 atm. Only the results corresponding to  $P = 1$  atm are presented here. Figure 3 illustrates the maximum flame temperatures of  $\text{H}_2/\text{CO}$  flame as a function of scalar dissipation rate at  $\text{H}_2/\text{CO} = 1.4$ , with and without the consideration of flame radiation. The inlet temperature is 300 K and ambient pressure is 1 atm. For the case without radiation, the result shows a monotonic trend of maximum flame temperature with respect to scalar dissipation rate. The flame temperature decreases with increasing scalar dissipation rate until the blowoff. The temperature reduction at higher scalar dissipation rate is the result of insufficient gas residence time. However, with radiation, the maximum flame temperature exhibits a peak at an intermediate scalar dissipation rate for a given value of  $\text{H}_2/\text{CO}$  ratio (at  $\chi \sim 10 \text{ s}^{-1}$ ). This result is different to the case without radiation, and this difference grows to be very large as scalar dissipation rate is decreased. The drop of the flame temperature at lower scalar dissipation rate is the result of increasing radiative loss. The flame extinction occurs at high stretch rate because of insufficient gas residence time for chemical reaction. Radiative heat loss is largely dependent upon

flame volume and the thickness of reaction zone is relevant to the reciprocal of scalar dissipation rate. As a result the difference of maximum flame temperatures with and without radiation becomes small with the increase of scalar dissipation rate. This trend has been also identified in previous studies [4]. The maximum flame temperatures of  $H_2/CO$  counterflow diffusion flames as a function of  $H_2/CO$  rate are depicted in figure 4. Flame temperatures increase more the syngas is  $H_2$ -rich for strain rates values below the intermediate value. The opposite behaviour is noticed for strain rate values higher than the intermediate value. The behaviour of maximum NO as a function of  $H_2/CO$  rates in figure 5 is similar to that of the maximum temperature (Fig. 4). NO mass fractions exhibit a monotonic increase with hydrogen enrichment at low values of the scalar dissipation rate. The opposite trend is noticed at high stretch values. This finding is concordant with the study of Drake and Blint [1] in which NO formation is found to be dominated by thermal route. Figure 6 presents  $EINO$  index as a function of scalar dissipation rate at  $P = 1$  atm.  $EINO$  index exhibits a non-monotonic variation with syngas composition. It increases to a maximum and then decreases. The scalar dissipation rate, at which the maximum  $EINO$  peaks, shifts toward lowest values with  $H_2$  enrichment. The peak of  $EINO$  index increases with hydrogen enrichment. An important observation from these results is the existence of operating conditions that yields lowest amount of NO production. Indeed, hydrogen-rich syngas flames produce more NO at lower scalar dissipation rates while NO levels increase towards hydrogen-lean syngas flames at higher scalar dissipation rate. In practice, Industrial combustion systems should operate at low scalar dissipations (near  $5 \text{ s}^{-1}$ ) with  $H_2$ -lean fuel or at very high scalar dissipations (between 100 and  $1000 \text{ s}^{-1}$ ) with  $H_2$ -rich syngas in order to minimize NO emissions. These findings agree with trends reported in the literature [6].

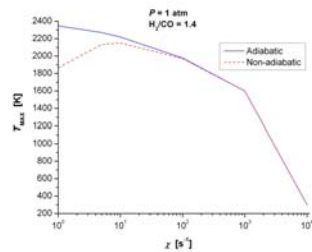


Figure 3. Maximum flame temperature as a function of scalar dissipation rate with and without flame radiation (1 atm, 300 K,  $H_2/CO = 1.4$ )

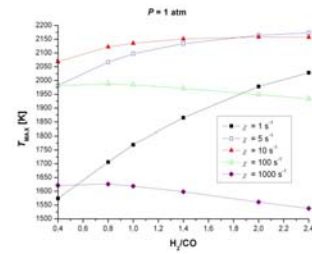


Figure 4. Maximum flame temperature as a function of scalar dissipation rate at different values of  $H_2/CO$  ratio (1 atm, 300 K)

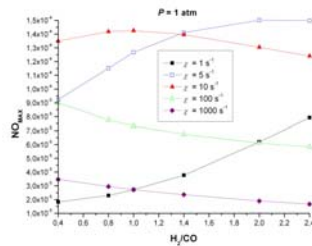


Figure 5. Maximum NO mole fraction as a function of scalar dissipation rate at different values of  $H_2/CO$  ratio (1 atm, 300 K)

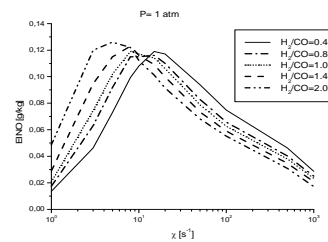


Figure 6. NO emission index as a function of scalar dissipation rate at different values of  $H_2/CO$  ratio (1 atm, 300 K)

## 4 Conclusion

This work is intended to provide some understanding of the effects of fuel variability and operating pressure on the structure and emissions of syngas flames. Optimum conditions corresponding to acceptable levels of NO emissions were also investigated. The maximum flame temperature exhibits a peak at an intermediate scalar dissipation rate for a given value of H<sub>2</sub>/CO ratio. For values of strain rate lower than the intermediate value, flame structure is influenced by combined effects of adiabatic temperature and radiation heat loss, whereas only adiabatic temperature effect exists at higher values of strain rate. The flame temperature increases more the syngas is H<sub>2</sub>-rich for strain rates values below the intermediate value mainly due to the decrease of flame radiative losses. Indeed, H<sub>2</sub> enrichment induced more H<sub>2</sub>O and less CO<sub>2</sub>. H<sub>2</sub>O emissions being less important than CO<sub>2</sub> emissions. In addition, H<sub>2</sub> enrichment reduces flame thickness. The opposite behaviour is noticed for the flame temperature at strain rate values higher than the intermediate value. NO<sub>x</sub> formation is closely related to flame temperature. Hydrogen-rich syngas flames produce more NO<sub>x</sub> at lower strain rates while NO<sub>x</sub> levels increase towards hydrogen-lean syngas flames at higher strain rates. Increasing pressure enhances NO<sub>x</sub> formation reactions, especially through Zeldovich mechanisms. In practice, Industrial combustion systems should operate at low scalar dissipations (near 5 s<sup>-1</sup>) with H<sub>2</sub>-lean fuel or at very high scalar dissipations (between 100 and 1000 s<sup>-1</sup>) with H<sub>2</sub>-rich syngas in order to minimize NO<sub>x</sub> emissions.

## References

- [1] Drake M.C., Blint R.J. (1989). *Combust. Flame* 76: 151–167.
- [2] Park J., Bae D.S., Cha M.S., Yun J.H., Keel S.I., Cho H.C., Kim T.K., Ha J.S. (2008). Flame characteristics in H<sub>2</sub>/CO synthetic gas diffusion flames diluted with CO<sub>2</sub>: Effects of radiative heat loss and mixture composition, *international journal of hydrogen energy* 33:7256 – 7264
- [3] Giles D.E., Som S., Aggarwal S.K. (2006). *Fuel* 85: 1729 - 1742.
- [4] Shih H-Y, Hsu J-R (2012). Computed extinction limits and flame structures of opposed-jet syngas diffusion flames, *Applied Mechanics and Materials* 110 – 116: 4899 - 4906.
- [5] Som S., Ramirez A.I., Hagerdorn J., Saveliev A., Aggarwal S.K. (2008). A numerical and experimental study of counterflow syngas flames at different pressures, *Fuel* 87: 319–334.
- [6] Shih H-Y, Hsu J-R. Computed NO<sub>x</sub> emission characteristics of opposed-jet syngas diffusion flames, *Combust. Flame*, article in press.
- [7] Chacartegui R., Sánchez D., Muñoz de Escalona J.M., Monje B., Sánchez T. On the effects of running existing combined cycle power plants on syngas fuel, *Fuel Processing Technology*, article in press
- [8] Chacartegui R., Torres M., Sánchez D., Jiménez F., Muñoz A., Sánchez T. (2011) Analysis of main gaseous emissions of heavy duty gas turbines burning several syngas fuels, *Fuel Processing Technology* 92: 213 – 220
- [9] Advanced Hydrogen Turbine Development” Factsheet, Project DE-FC26-05NT42644, National Energy Technology Laboratory, U.S. Department of Energy, 2006.
- [10] Geyer D., Dreizler A. *et al.* (2005). Finite-rate chemistry effects in turbulent opposed flows: comparison of Raman/Rayleigh measurements and Monte Carlo PDF simulations, *Proc. Combust. Inst.*,30: 711-718.
- [11] Pitsch H., Peters N. (1998). Consistent flamelet formulation for nonpremixed combustion considering differential diffusion effects, *Combust Flame* 114: 26 - 40.
- [12] N. Peters, *Turbulent combustion*, Cambridge University Press, 2000.
- [13] R.S. Barlow, N.S.A. Smith, J.Y. Chen, R.W. Bilger, Nitric Oxide formation in dilute hydrogen jet flames: isolation of the effects of radiation and turbulence-chemistry submodels, *Combust Flame* 117(1999) 4 - 31.
- [14] Modest MF. *Radiative heat transfer*, Mechanical and technical engineering, 2nd ed. New York: Academic Press; 2003.